



# Using beryllium-7 to evaluate soil erosion processes in agricultural lands in semiarid regions of Central Argentina

Juan Pablo de Rosas<sup>1,2</sup> · Alexander Dario Esquivel<sup>3</sup> · Diego Martinez Heimann<sup>4</sup> · Agustin E. Negri<sup>4</sup> · Flavia Lohaiza<sup>1</sup> · Diego Leonardo Valladares<sup>1,2</sup> · Alejandro I. Zavala<sup>5</sup> · Hugo Huck<sup>5,6</sup> · Jimena Juri Ayub<sup>1,7</sup>

Received: 30 November 2017 / Accepted: 16 August 2018  
© Springer-Verlag GmbH Germany, part of Springer Nature 2018

## Abstract

This work presents the results of a soil erosion study using the <sup>7</sup>Be technique. This technique estimates the water erosion/deposition from the comparison between <sup>7</sup>Be soil content of a reference site and an eroded or sedimented site. The soil samples were collected from an agricultural area of the semiarid region of Argentina near San Luis City, which has a marked rainfall season. The area has been used for crop cultivation, being subjected to plowing practices. The <sup>7</sup>Be in the Reference Site was in the first centimeter of soil, showing the typical exponential decreasing of <sup>7</sup>Be soil content with depth, with the <sup>7</sup>Be inventories value being  $340 \pm 50 \text{ Bq m}^{-2}$  for the dry season and  $571 \pm 48 \text{ Bq m}^{-2}$  for the rainy season. The <sup>7</sup>Be technique was applied to a potential eroded site subjected to traditional tillage practices (plowing). A net soil erosion value of  $13.5 \text{ t ha}^{-1}$  ( $1.35 \text{ kg m}^{-2}$ ) was obtained. From the assumptions of the applied technique, we can draw the inference that this erosion was caused by rains produced in the month prior to the date of soil sampling.

**Keywords** Soil degradation · Soil tillage · Radiotracer · Gamma spectrometry · Fallout radionuclide

## Introduction

Beryllium-7 (<sup>7</sup>Be) is a cosmogenic radionuclide with a half-life of 53.3 days produced in the atmosphere by cosmic ray spallation of nitrogen and oxygen atoms (Lal et al. 1958; Ioannidou and Papastefanou 2006). About 75% of <sup>7</sup>Be is produced in the stratosphere and 25% in the upper troposphere

(Yoshimori 2005). This radionuclide decays by electron capture in two ways, 89.5% of <sup>7</sup>Be atoms decay directly to the ground state of stable isotope of lithium (<sup>7</sup>Li) and 10.5% decays first to a metastable isotope (<sup>7</sup>mLi). The half-life of <sup>7</sup>mLi is short, decaying immediately, via gamma ray emission at 477.6 keV, to ground state <sup>7</sup>Li (Kaste et al. 2002).

Several factors affect the <sup>7</sup>Be flux that reaches the Earth's surface. The incoming cosmic rays at the upper atmosphere are deflected by both the Sun's heliosphere and Earth's magnetosphere. The <sup>7</sup>Be production varies with the 11-year solar cycle (Papastefanou and Ioannidou 2004;

This article is a part of Topical Collection in Environmental Earth Sciences on IV RAGSU—Advances in Geochemistry of the Surface in Argentina, edited by Dr. Americo Iadran Torres and Dr. Pablo Jose Bouza.

✉ Jimena Juri Ayub  
jjuri@unsl.edu.ar

- 1 Grupo de Estudios Ambientales – Instituto de Matemática Aplicada San Luis – Universidad Nacional de San Luis/ CCT-San Luis, CONICET, Ejército de los Andes 950, San Luis Capital, San Luis, Argentina
- 2 Departamento de Física, Universidad Nacional de San Luis, Ejército de los Andes 950, San Luis Capital, San Luis, Argentina
- 3 Centro de Investigaciones Hidráulicas e Hidrotécnicas (CIHH), Universidad Tecnológica de Panamá, Vía Domingo Díaz al lado de Pazco, S.A., El Dorado, Panama

<sup>4</sup> Instituto de Investigación e Ingeniería Ambiental, Universidad Nacional de San Martín, CONICET, 25 de Mayo y Francia, B1650BWA San Martín, Buenos Aires, Argentina

<sup>5</sup> Departamento de Física Experimental, Comisión Nacional de Energía Atómica, Av. Gral. Paz 1499, 1650, B1650BWA San Martín, Buenos Aires, Argentina

<sup>6</sup> Escuela de Ciencia y Tecnología, Universidad Nacional de San Martín, 25 de Mayo y Francia, B1650BWA San Martín, Buenos Aires, Argentina

<sup>7</sup> Departamento de Bioquímica y Ciencias Biológicas, Universidad Nacional de San Luis, Ejército de los Andes 950, San Luis Capital, San Luis, Argentina

Van Allen 2000; Piñero García and Ferro García 2013). The  $^7\text{Be}$  flux reaching the Earth's surface is determined by its atmospheric production rate, stratosphere–troposphere mixing and tropospheric circulation, giving rise to the observation that the  $^7\text{Be}$  flux is dependent on latitude, longitude, and azimuth angle (Kaste et al. 2002).

Immediately after its production,  $^7\text{Be}$  is oxidized into beryllium oxide and adheres to aerosols. These aerosols are transported to lower levels of the atmosphere and from there they are deposited on the Earth's surface by wet and dry fallout (Kaste et al. 2002; Papastefanou 2006). Several authors have reported that the main mechanism of  $^7\text{Be}$  deposition is wet deposition (rain and snow) and that dry deposition contributes less than 10% to the total deposition (Salisbury and Cartwright 2005; Ioannidou and Papastefanou 2006; Wallbrink and Murray 1994). Furthermore, it can be assumed that the atmospheric concentration of  $^7\text{Be}$  over a small area will be essentially uniform at a given time (Doering et al. 2006).

The short half-life of  $^7\text{Be}$ , its continuous production rate, and the easy detection by gamma spectrometry makes  $^7\text{Be}$  a powerful tool for surveying environmental processes. Beryllium-7 has been used to estimate soil redistribution, sediment source discrimination, trace metal scavenging from the atmosphere and atmospheric mass transport (Kaste et al. 2002; Yoshimori 2005; Steinmann et al. 1999; Daish et al. 2005; Matissoff et al. 2002; Walling et al. 1999; Blake et al. 1999; Schuller et al. 2006; Sepulveda et al. 2008). In regard to erosion estimation, Kaste et al. (2011) pointed out that most of the  $^7\text{Be}$  erosion estimates were made in environments having moderate or a well-balanced supply of moisture, and there is a lack of published work in arid environment.

In the present research, we evaluate soil erosion in an area situated in a semiarid region of Central Argentina (San Luis Province), characterized by a marked seasonality in the rainfall regime, with a dry season in autumn and winter months and a wet season in spring and summer months. The region is located in the expansive frontier of agricultural development, with its native vegetation (shrub forest and natural grassland) replaced by commercial crops (soybean, corn). Practices developed for decades in the humid Pampas have moved to semiarid and arid environments without making clear the environmental consequences derived from them, particularly with regard to soil degradation processes (FAO 2013). The changes in the land use can lead to several consequences in the environment, particularly with regard to soil degradation, and a quick and efficient tool is essential to verify if land degradation takes place. With the aim of exploring the applicability of  $^7\text{Be}$  as a tracer of soil redistribution in a semiarid environment, the technique was used to estimate erosion in a farm where soil is periodically plowed.

## Materials and methods

### Study area and rainfall seasonality

The study area is located 20 km south-east of San Luis City (S 33.3153°; W 66.1010°, 1020 m a.s.l.) in an agricultural region, namely *La Cumbre* (Fig. 1). According to Knöppen classification, the climate is semi – arid. The region has two distinct seasons: a warm and rainy season from October to March and a cool and dry season from April to September. The monthly average temperatures vary between 9 and 23 °C.

To apply the  $^7\text{Be}$  technique, reliable rainfall data are needed because the rain is both the main source of  $^7\text{Be}$  input to the soil and the erosive factor. Two rainfall databases with the data of the study area were analyzed in this study. One data set was obtained from the Weather Station Network of the San Luis Province (REM 2017). The second source of rainfall data was obtained from the Tropical Rainfall Measuring Mission (TRMM, which ended in 2014) and the Global Precipitation Measurement Mission (Huffman et al. 2017). For simplicity, the second data set is referred to as TRMM in this work.

The REM has around 80 weather stations in San Luis Province, providing a variety of climate data. The nearest network's station is 4 km away from the study area (S 33.3424°; W 66.1212°), named station REM La Cumbre. The database has rainfall data beginning at the end of 2007 until the present day, with hourly resolution. In this work, the rainfall data set was integrated (cumulated) over time periods of 24 h to achieve daily resolution.

The rainfall data of TRMM correspond to algorithm version 3B42RT (Huffman 2015). These multi-satellite data are gridded estimates of rain rate on a daily temporal resolution and a  $0.2500^\circ \times 0.2500^\circ$  spatial resolution. Different source data (satellite and rain gauges) are processed algorithmically to obtain one temporal series. The time series was downloaded from the Giovanni platform (Giovanni 2017). The standard Giovanni time series data are produced by computing the spatial averages over the user-selected area of a given variable for each time step within the user's range. For the computation of the rainfall time series, a precipitation average was calculated in the region limited by the bounding box (W 66.2500°; S 33.4000° and W 66.0000°; S 33.0500°), which includes both the study area and the REM La Cumbre.

Figure 2 shows the mean monthly precipitation obtained from both REM and TRMM, for a 9 year period (2008–2016). Both data sets display the same rainfall regime, with the rainy season between October and March, and the dry season between April and September. The accumulated mean annual precipitation is  $641 \pm 132$  mm from REM and  $778 \pm 185$  mm from TRMM.

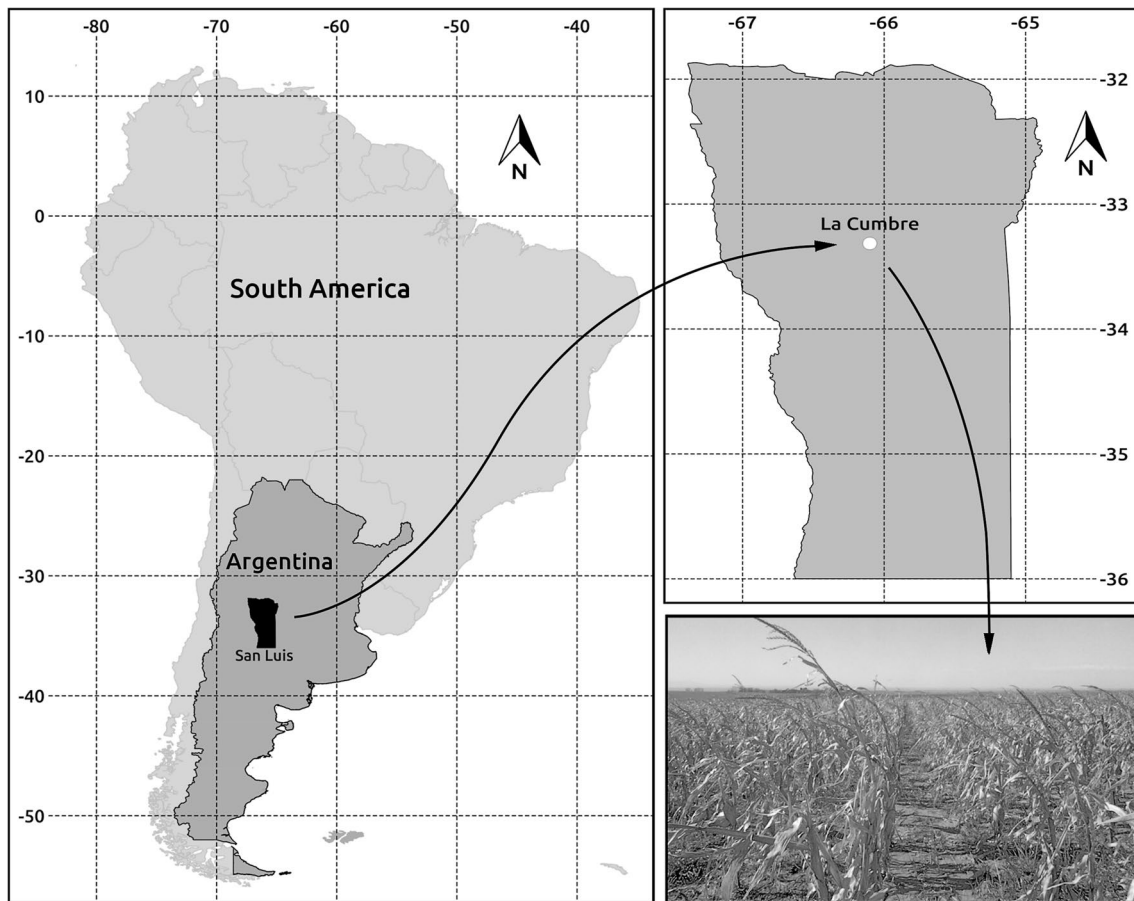


**Fig. 1** Location of the study area. Photograph of the Study Site with corn plants

The strong seasonal behavior of the rains is clearly visualized in both data sets; 85% of the accumulated precipitation falls in the rainy season for the two data sets REM and TRMM. Nevertheless, differences in the monthly precipitation are recorded between both databases; TRMM annual value is 1.2 times greater than the REM value. Fengge et al. (2007) report that the TRMM data set overestimates the precipitation amount through the increase of the number of rainfall events that take place and the rise of the amount of fallen millimeters in each rain event. For the study area, the TRMM overestimation seems to be stronger in the rainy season, according to the report by Magliano et al. (2015). Therefore, the REM data set was used throughout this work.

### Soil sampling and gamma spectrometry analysis

In the study area, two nearby sites were selected. The first site, named Study Site, is plowed periodically and used for soybean and corn cultivation (Fig. 1), having average slopes from 3 to 5%. The second site, named Reference Site, is flat (slope  $\approx 0$ ), without evidence of soil redistribution (erosion and/or sedimentation). This site has not been plowed for at

least the last 5 years (landlord personal communication) and is expected to show an exponential decreasing  $^7\text{Be}$  content with incremental depth (Zapata 2002).

Two campaigns for soil sampling were made. The first campaign was a preliminary study, with the aim of knowing the  $^7\text{Be}$  soil content values (inventory), its vertical soil distribution and the viability to reliably measure this radionuclide in both the available laboratory and experimental conditions. This sampling campaign was carried out on September 16, 2016 (ending of the dry season). In this instance, three sampling points were marked (named FC1, FC2 and FC3) over a transect parallel to the slope (east–west direction) in the Study Site. The points were located in the upper (FC1), middle (FC2) and lower (FC3) parts of the slope. In the Reference Site, one sampling point was marked. From each sampling point, three soil profiles were collected without disturbances (see below).

The second sampling campaign was on June 17, 2017. At this time, a transect about 460 m long, in east–west direction, was marked in the Study Site. Over this transect, ten sampling points were marked (named SC1, SC2, ..., SC10), with inter-point distances of 30 or 60 m. In the Reference

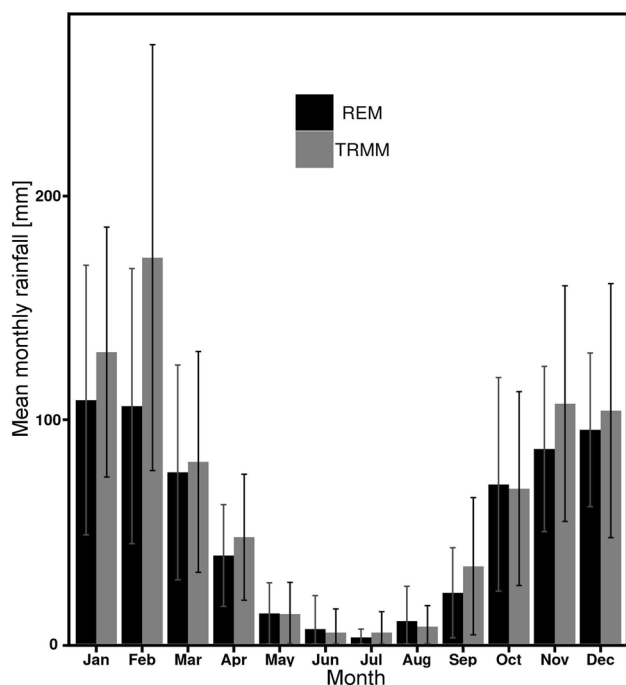


**Fig. 2** Mean monthly precipitation for a 9-year period (2008–2016), for both rainfall data sets (REM and TRMM). The error bars are standard deviation

Site, three sampling points were marked. In each sampling point, three soil profiles were collected without disturbances (see below).

For the soil profile extraction, plastic tubes (10.6 cm diameter  $\times$  5 cm height) were used. The plastic tubes were driven into the soil avoiding any possible disturbance. Once in the laboratory, each soil profile was sliced per 2 or 4 mm increments, for the 2 cm topsoil. Soil samples from the same layer and same sampling point were mixed, dried on stove (60 °C) to constant weight, sieved through a 2 mm mesh and packed for further gamma spectrometry analysis.

In the soil samples, the  $^7\text{Be}$  activity concentration was determined by gamma spectrometry, measuring the gamma emission at 477.6 keV. The gamma spectrometer is a high purity germanium crystal with a carbon fiber window that allows for measurements from 5 keV upward, built by ORTEC. The detector is located at the Tandem Laboratory (Comisión Nacional de Energía Atómica, Centro Atómico Constituyentes, Buenos Aires Province). The energy resolution was 1.9 keV at 1.3 MeV. The detector was surrounded by lead bricks to provide shielding from the radioactive background. Absolute photo-peak detection efficiency measurement was performed following the method proposed by Perillo Isaac et al. (1997). We used a mixture of the naturally occurring long-lived isotopes,  $^{176}\text{Lu}$ ,  $^{138}\text{La}$ , and  $^{40}\text{K}$ . These isotopes emit gamma rays with energies ranging from 88 to 1460 keV and have simple and well-understood decay

schemes. The calibration source was prepared by mixing known amounts of the chemical compounds  $\text{Lu}_2\text{O}_3$ ,  $\text{La}_2\text{O}_3$ , and KCl in a matrix of soil. To monitor the environmental radiation, room background was periodically measured. The data were acquired using standard electronic instruments, recorded in an 8K ADC (analog-digital converter) multi-channel analyzer based on a personal computer. The counting period for the samples was 24 h, to diminish statistical counting fluctuations. The gamma spectra were analyzed for all samples to obtain the area of the 477.6 keV peak. The measured activities were corrected to the time of the sample collection. The background count rate was 0.001 counts/s/keV at the region of interest. All uncertainties ranged from 10% for the topsoil slices (which usually have higher activity concentrations), to 50% for the slices with low activity concentration of  $^7\text{Be}$  with activities around 5 Bq/kg. This value is approximately the detection limit of our measurements in this work.

### $^7\text{Be}$ soil content and soil redistribution

For sites where the soil is unperturbed, it has been found that the  $^7\text{Be}$  activity concentration  $C(x)$  [ $\text{Bq kg}^{-1}$ ] has an exponential decrease with soil mass depth  $x$  (positive downward) [ $\text{kg m}^{-2}$ ]. Soil mass depth is used to measure depth in soil and is defined as the product of the soil bulk density and the depth of soil layer. Therefore,  $C(x)$  can be expressed as:

$$C(x) = C(0)e^{(-x/h_0)}, \quad (1)$$

where  $C(0)$  is the activity concentration on the soil surface. The parameter  $h_0$  is named the relaxation mass depth and is used to quantify the  $^7\text{Be}$  penetration into soil. The exponential behavior of  $^7\text{Be}$  concentration in unperturbed soils has been confirmed by many field experiments (Sepulveda et al. 2008; Walling et al. 2009; Lohaiza et al. 2014).

Taking into account the distribution defined by Eq. (1), the areal activity density  $A(x)$  [ $\text{Bq m}^{-2}$ ] is defined as follows:

$$A(x) = \int_x^\infty C(x) dx = A_{\text{ref}} e^{(-x/h_0)}. \quad (2)$$

The total areal activity density  $A_{\text{ref}}$  [ $\text{Bq m}^{-2}$ ] is the  $^7\text{Be}$  soil inventory. According to Eq. (1),  $A_{\text{ref}}$  can be calculated as:

$$A_{\text{ref}} = \int_0^\infty C(x) dx = h_0 C(0). \quad (3)$$

Measuring the activity concentration  $C(x)$  in each layer of sliced soil cores for the reference site, it is possible to calculate  $A(x)$ , and thus estimate the parameters  $A_{\text{ref}}$  and  $h_0$  by regression of data with the model described by Eq. (2).

Unlike the reference sites, soil profiles in the study sites do not necessarily exhibit an exponential decrease of  $A(x)$  as a function of  $x$ . This is due to soil movements, which transport the  $^7\text{Be}$  adhered to soil particles, changing the initial  $^7\text{Be}$  distribution. Therefore, the eroded sites will present  $^7\text{Be}$  inventories lower than the reference sites and decapitated soil profiles. On the other hand, the sedimented sites will present higher inventories than reference sites and buried soil profiles.

The differences in  $^7\text{Be}$  inventory between the reference sites and study sites can be used to estimate the eroded/sedimented soil mass per unit area in the study sites, in  $\text{kg m}^{-2}$ . These calculations were made using the conversion model proposed by Sepulveda et al. (2008).

## Results and discussion

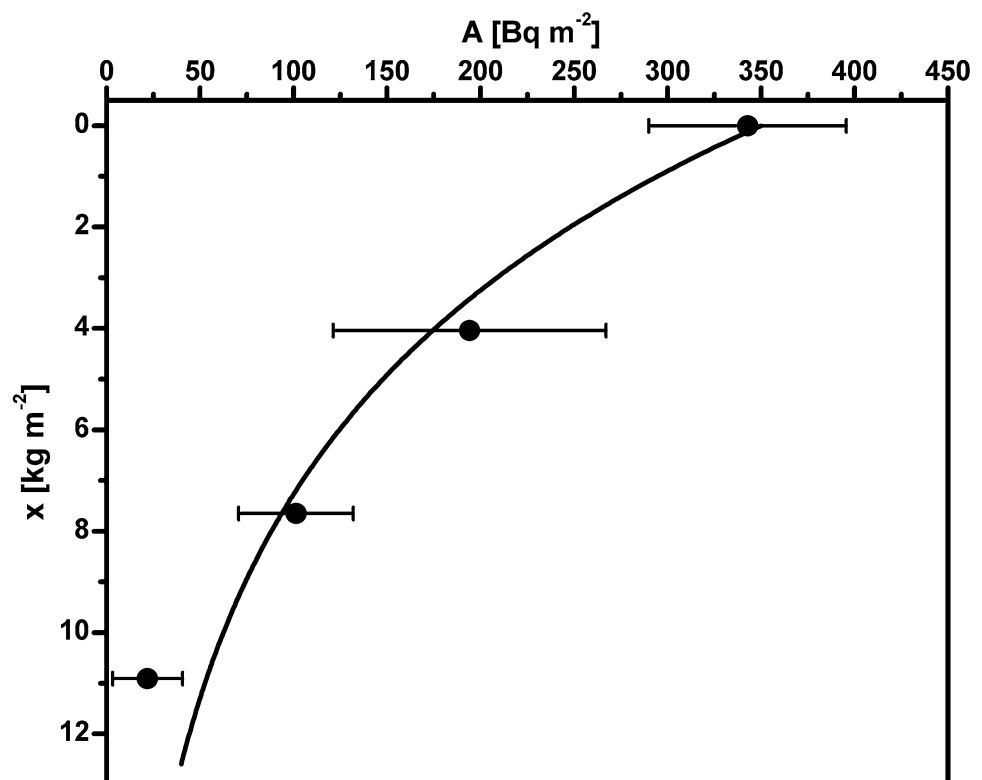
As explained above, to estimate soil erosion using the  $^7\text{Be}$  technique, a preliminary sampling campaign was carried out on September 16, 2016. During this campaign, potential reference and study sites were evaluated. In each site, soil samples were taken without disturbances.

For the site chosen as the reference site (Reference Site), the measured  $^7\text{Be}$  inventory was  $340 \pm 50 \text{ Bq m}^{-2}$  and its  $^7\text{Be}$  vertical distribution in soil shows the vertical profile displayed in Fig. 3 (circles). For regions of southern Chile characterized by precipitation almost uniformly distributed

along the year, Schuller et al. (2006) report  $^7\text{Be}$  inventory of  $564 \pm 60 \text{ Bq m}^{-2}$  (annual precipitation of 2300 mm) and Sepulveda et al. (2008) report  $499 \pm 10 \text{ Bq m}^{-2}$  (annual precipitation of 1100 mm). Kaste et al. (2011) for a region in USA with well-defined dry and rainy season (annual precipitation of 750 mm) report  $^7\text{Be}$  inventories values between  $29 \pm 2.6$  and  $383 \pm 59 \text{ Bq m}^{-2}$  (November 2006 to May 2010). Lohaiza et al. (2014), in a nearby region of San Luis Province (40 km south of our site, annual precipitation of 509 mm), report inventory values between  $51 \pm 25$  and  $438 \pm 114 \text{ Bq m}^{-2}$  (monthly sampling between the years 2009 and 2010). The measured  $^7\text{Be}$  inventory in the Reference Site is in the expected range for a humid period, despite the fact that the date corresponds to the end of the dry season. This is because there are some rainy days prior to the sampling date (see below).

With respect to the vertical distribution of  $^7\text{Be}$  in soil, the measured distribution shows that the  $^7\text{Be}$  is retained in the uppermost millimeters of soil, reaching 0.8 cm of the soil profile (Fig. 3). This superficial penetration of  $^7\text{Be}$  in soils has been reported for other areas of this arid region (Lohaiza et al. 2014) and several regions of the continent (Sepulveda et al. 2008; Schuller et al. 2006). Furthermore, it is observed that  $^7\text{Be}$  areal activity density ( $A(x)$ ) shows an exponential decrease with increasing mass depth, a typical behavior of undisturbed soil of reference sites. Figure 3 also shows (continuous line) the curve obtained by a nonlinear regression of  $A(x)$  with the model described by Eq. (2). The

**Fig. 3**  $^7\text{Be}$  soil content  $A(x)$  [ $\text{Bq m}^{-2}$ ] as a function of mass depth  $x$  [ $\text{kg m}^{-2}$ ] (circles) in the reference site, on September 16, 2016. The curve obtained by fitting with Eq. (2) (line). The error bars represent measurement error



fitted parameter values obtained are  $A_{\text{ref}} = 350 \pm 78 \text{ Bq m}^{-2}$  and  $h_0 = 5.8 \pm 2.6 \text{ kg m}^{-2}$  ( $R^2 = 0.97$ ). The model of Eq. (2) predicts the vertical distribution of  $^7\text{Be}$  areal activity density for this sampling place; it explains at least 90% of the variability in the measured data.

The relaxation mass depth  $h_0$  value characterizes the penetration of the radionuclide into the soil. Lohaiza et al. (2014) report relaxation mass depth values ranging 1.2–2.9  $\text{kg m}^{-2}$ . In a region of the south of Chile, Sepulveda et al. (2008) published an  $h_0$  value of  $3.4 \pm 0.1 \text{ kg m}^{-2}$ , while Schuller et al. (2006) obtained a value for relaxation mass depth of  $h_0 = 2.14 \text{ kg m}^{-2}$ . Esquivel et al. (2017), measuring in Minas Gerais, Brazil, found an unusual relaxation mass depth of  $43.4 \text{ kg m}^{-2}$ . The wide range of reported values for  $h_0$  could be explained by the dependence of this parameter on several soil properties, such as the drainage structure, chemical composition and moisture status of the soil (Sepulveda et al. 2008; Kaste et al. 2002). From the information provided by the farmer and measurement results, we can conclude that this site could be used as a reference site for soil redistribution studies using the  $^7\text{Be}$  technique.

Figure 4a displays the areal activity density  $A(x)$  as a function of mass depth  $x$  for the three soil profiles sampled in the Study Site (FC1, FC2 and FC3) on September 16, 2016 (first sampling campaign). Figure 4b shows the relative height of these sampling points (0 m at 1010 m a.s.l.), which are located along a transect whose average slope is 5%. The  $^7\text{Be}$  inventories were  $240 \pm 80 \text{ Bq m}^{-2}$ ,  $380 \pm 90 \text{ Bq m}^{-2}$  and  $440 \pm 30 \text{ Bq m}^{-2}$  for FC1, FC2 and FC3, respectively. Only

FC2 shows a  $^7\text{Be}$  inventory equivalent to that registered in the Reference Site ( $340 \pm 50 \text{ Bq m}^{-2}$ ), with the  $^7\text{Be}$  inventory value of FC3 greater than the inventory of the Reference Site. The changes in the  $^7\text{Be}$  inventory across the transect could be explained by the transport of soil particles, with adhered  $^7\text{Be}$ , downhill due to the height of the terrain.

With this result in mind and with the aim of quantifying the erosion using  $^7\text{Be}$  in the Study Site, a second sampling campaign was carried out on June 17, 2017. Figure 5 shows  $A(x)$  vs.  $x$  as circles for the Reference Site at the time of sampling. In the same way as for the date of the preliminary study, the  $^7\text{Be}$  is present in the uppermost millimeters of soil, reaching 1 cm depth, and the  $^7\text{Be}$  activity also seem to decrease exponentially with depth. The  $^7\text{Be}$  inventory is  $570 \pm 80 \text{ Bq m}^{-2}$ , with this value being 1.7 times greater than the measurement made in September 2016. The difference between both values could be explained by the rainfall regime. The  $^7\text{Be}$  inventory in September is expected to be lower, corresponding to the last days of the dry season, while June month is closer in time to the rainy season. Furthermore, in 2017 several rain events occurred between April and May, supplying  $^7\text{Be}$  to the soil from the atmosphere (see below). Figure 5 also shows the curve obtained by nonlinear regression of  $A(x)$  with the model described by Eq. (2). The parameters obtained in the fitting process are  $A_{\text{ref}} = 571 \pm 48 \text{ Bq m}^{-2}$  and  $h_0 = 3.6 \pm 0.5 \text{ kg m}^{-2}$  ( $R^2 = 0.99$ ). The exponential decrease model shows a good correlation with the experimental data, reconfirming the choice of the Reference Site.

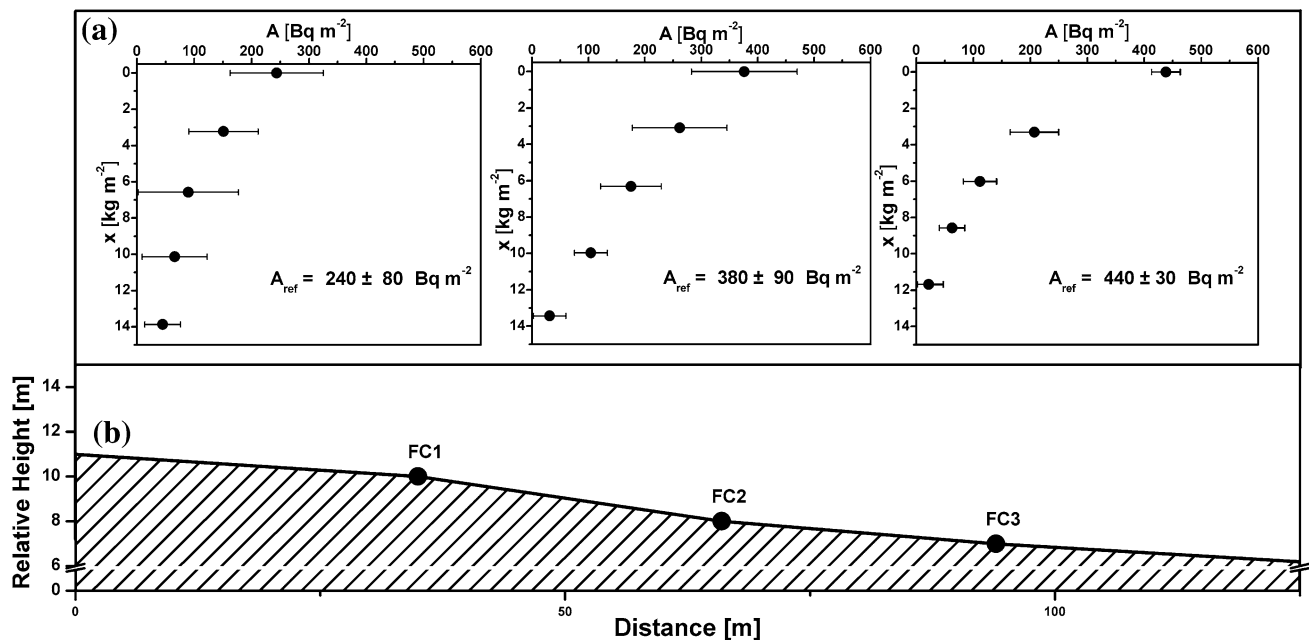


**Fig. 4**  $^7\text{Be}$  soil content  $A(x)$  [ $\text{Bq m}^{-2}$ ] as a function of mass depth  $x$  [ $\text{kg m}^{-2}$ ] in the three sampling points **a** along the transect, **b** in the study site, on September 16, 2016. 0 m is taken at 1010 m a.s.l

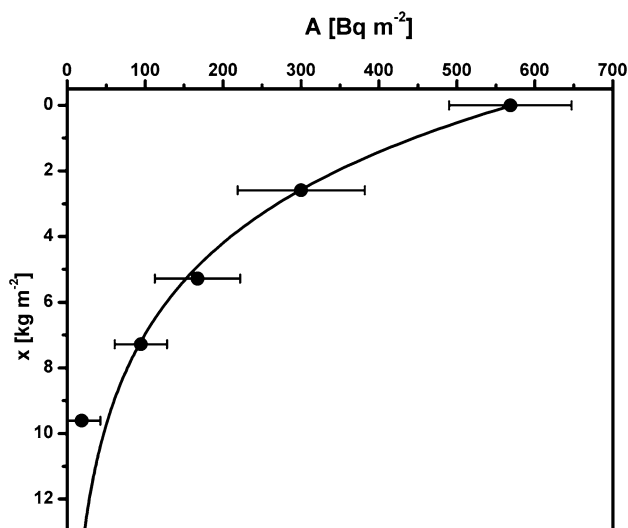


**Fig. 5** Average  ${}^7\text{Be}$  soil content  $A(x)$  [ $\text{Bq m}^{-2}$ ] as a function of mass depth  $x$  [ $\text{kg m}^{-2}$ ] (circles) in the Reference Site on June 17, 2017. Curve obtained by fitting with Eq. (2) (line). The error bars represent the standard deviation

To quantify the water erosion at the study site, soil samples were taken along a transect as explained above. Figure 6a shows the difference of the  ${}^7\text{Be}$  inventory between each sampling point in the Study Site and the Reference Site. Figure 6b shows the relative height of the ten sampling points at the Study Site (0 at 1010 m a.s.l.). Across the

transect only one sampling point (SC3) has a  ${}^7\text{Be}$  inventory value greater than the  ${}^7\text{Be}$  inventory value of the Reference Site, indicating that this is a point of soil sedimentation. For all other sampling points on the transect, the  ${}^7\text{Be}$  inventories are lower than the inventory of the Reference Site, indicating that there is soil erosion in this points. This last result is expected due to the location of the sampling points over a downhill transect.

The erosion is commonly ranked into several categories, according to  $\text{kg ha}^{-1}$  of soil loss by year, as light (weak) erosion ( $< 20 \text{ t ha}^{-1}$ ), moderate erosion ( $20\text{--}100 \text{ t ha}^{-1}$ ), heavy erosion ( $100\text{--}300 \text{ t ha}^{-1}$ ) and severe erosion ( $> 300 \text{ t ha}^{-1}$ ). The region of Argentina where it is located, the Study Site has been classified as a region subject to both wind and water erosion (Casas 2001), and GLADIS maps from the LADA Project of FAO characterize the region as subject to slightly negative process of degradation with a slow acceleration of the degradation rate (Nachtergaele et al. 2011).

The  ${}^7\text{Be}$  technique does not estimate annual mean erosion; the mass of soil lost or gained estimated by this technique is attributed to the rainfall events that take place before the measurements. Using the model described by Sepulveda et al. (2008) for the study site, a net erosion of  $13.5 \text{ t ha}^{-1}$  ( $1.35 \text{ kg m}^{-2}$ ) was calculated. This erosion value indicates that an upper soil layer of 1.3 mm thickness was lost. Figure 7a shows the rains that occurred in the last 100 days before the soil sampling date (June 17, 2017 is the 0 day in Fig. 7a). We can observe that there are 11 days of rainfall

**Fig. 6**  $\Delta I$  equal to difference between  ${}^7\text{Be}$  soil inventory of each sampling point and the  ${}^7\text{Be}$  soil inventory of the Reference Site ( $571 \pm 48 \text{ Bq m}^{-2}$ ) on June 17, 2017 (a); along the transect (b). The 0 m is taken at 1010 m a.s.l

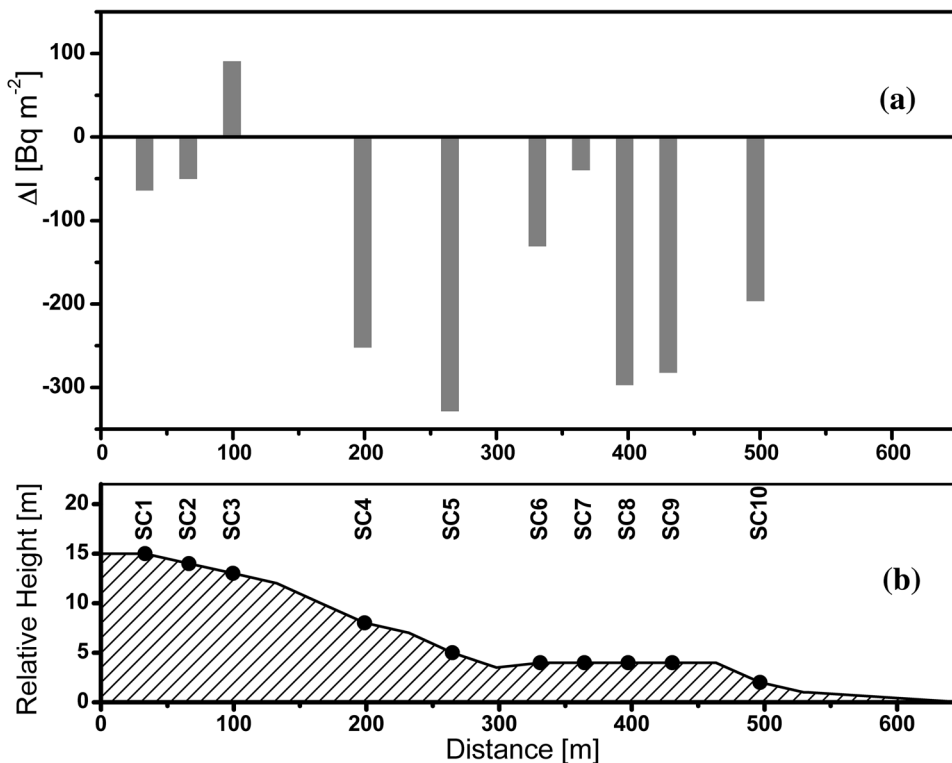
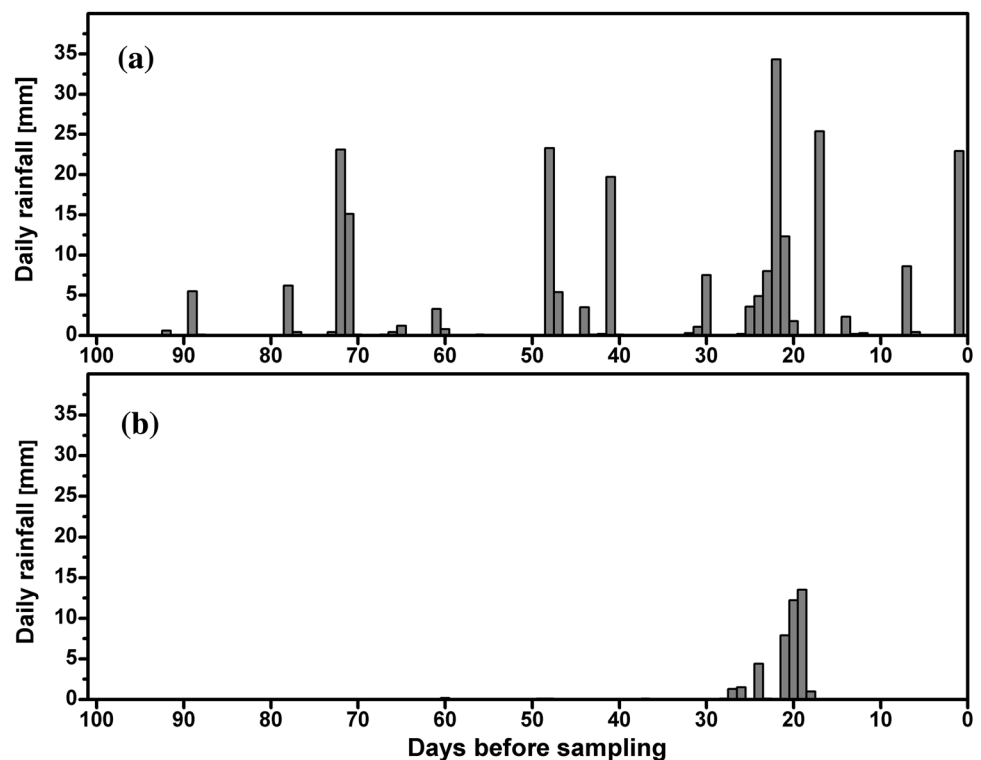


**Fig. 7** Daily rainfall [mm] 100 days before the soil sampling time: 0 is June 17, 2017 (a) and September 16, 2016 (b). Rainfall data obtained from REM La Cumbre



during the 25-day period prior to soil sampling, three of them have magnitudes greater than 20 mm and one reaches over 35 mm. These heavy rains could be taken as the main erosion events that cause erosion with the estimated erosion value of  $13.5 \text{ t ha}^{-1}$ . If this erosion value is simply extrapolated to the year, the  $^7\text{Be}$  technique would show that during this period the soil loss values are in the range from weak to moderate erosion.

Also, we calculate the erosion value using the  $^7\text{Be}$  inventories recorded in the preliminary study (first campaign). In this case, a net erosion value of  $1.70 \text{ t ha}^{-1}$  ( $0.17 \text{ kg m}^{-2}$ ) was obtained, lesser than that reported for the second campaign. Figure 7b shows the rain events that occurred during 100 days prior to the sampling date of the first campaign (September 16, 2016 is day 0). It could be observed that, in the dry season, small and scarce rain events occurred. This could explain the difference in the net erosion values obtained for the two campaigns.

## Conclusions

The performed study shows that the  $^7\text{Be}$  technique is useful to estimate the erosion of soil produced by rain, in an area with semiarid climate and well-defined rainy seasons. For this research, an area subjected annually to plowing practices for corn and soybean crop, with a moderate slope (3–5%) was chosen as the study site. Two soil sampling campaigns

were made. The first campaign allowed us mainly to verify the exponential decrease of  $^7\text{Be}$  content with soil depth in the potential reference site and to confirm our ability to measure the concentration of  $^7\text{Be}$  in soil with the precision required by the technique. The main results obtained show a net soil erosion of  $13.5 \text{ t ha}^{-1}$  ( $1.35 \text{ kg m}^{-2}$ ), corresponding to a superficial layer of 1.3 mm of soil that was lost in a short period of the time. The erosion was caused by rain events that took place in the month prior to the soil sampling. It is erroneous to obtain an annual erosion rate from the estimated erosion value, since this value corresponds to rainfall events produced within a month with particular rainfall conditions. Then, it is not possible to compare the value of the erosion obtained with those reported for the region, since these are reported as erosion rates per year. If in spite of this, if the erosion value obtained is used to obtain an annual erosion rate, the erosion rate per year is  $160 \text{ t ha}^{-1}$ . This erosion rate value assigns the study area to the category of moderate to severe erosion, needing prevention and restoration actions.

A complementary study using  $^{137}\text{Cs}$  as a soil erosion tracer would be necessary to provide definitive findings on this erosion value and an annual rate of loss soil mass.

**Acknowledgements** This research was supported by the Argentine institutions: the Universidad Nacional de San Luis (UNSL), the Consejo Nacional de Investigaciones Científicas y Técnicas (CONICET), the Universidad Nacional de San Martín (UNSAM) and the Comisión Nacional de Energía Atómica (CoNEA). The authors thank



the comments provided by the anonymous referees and the editor that greatly enriched this work.

## References

- Blake WH, Walling DE, He Q (1999) Fallout Beryllium-7 as a tracer in soil erosion investigations. *Appl Radiat Isot* 51(5):599–605. [https://doi.org/10.1016/S0969-8043\(99\)00086-X](https://doi.org/10.1016/S0969-8043(99)00086-X)
- Casas RR (2001) La Conservación de los Suelos y la Sustentabilidad de los Sistemas Agrícolas. Dissertation. Academia Nacional de Agronomía y Veterinaria. [http://sedici.unlp.edu.ar/bitstream/handle/10915/30748/Documento\\_completo.pdf?sequence=1](http://sedici.unlp.edu.ar/bitstream/handle/10915/30748/Documento_completo.pdf?sequence=1). Accessed 15 Mar 2017
- Daish SR, Dale AA, Dale CJ, May R, Rowe JE (2005) The temporal variations of  $^7\text{Be}$ ,  $^{210}\text{Pb}$  and  $^{210}\text{Po}$  in air in England. *J Environ Radioact* 84:457–467. <https://doi.org/10.1016/j.jenvrad.2005.05.003>
- Doering C, Akber R, Heijnis H (2006) Vertical distributions of  $^{210}\text{Pb}$  excess,  $^7\text{Be}$  and  $^{137}\text{Cs}$  in selected grass covered soils in Southeast Queensland. *Aust J Environ Radioact* 87:135–147. <https://doi.org/10.1016/j.jenvrad.2005.11.005>
- Esquivel AD, Moreira RM, Monteiro RPG, Dos Santos AAR, Juri Ayub J, Valladares DL (2017) Wet deposition and soil content of Beryllium-7 in a micro-watershed of Minas Gerais (Brazil). *J Environ Radioact* 169–170:56–63. <https://doi.org/10.1016/j.jenvrad.2016.12.014>
- FAO (2013) Land degradation assessment in dry lands, food and agriculture organization of the United Nations (2013). Report. E-ISBN 978-92-5-107567-8
- Fenge S, Hong Y, Lettenmaier DP (2007) Evaluation of TRMM multi-satellite precipitation analysis (TMPA) and its utility in hydrologic prediction in the La Plata basin. *J Hydrometeorol* 9(4):622–640. <https://doi.org/10.1175/2007JHM944.1>
- Giovanni (2017) The bridge between data and science, v. 4.24. <https://giovanni.gsfc.nasa.gov/giovanni/>. Accessed 15 Mar 2017
- Huffman G (2015) The transition in multi-satellite products from TRMM to GPM (TMPA to IMERG) 2015. [https://pmm.nasa.gov/sites/default/files/document\\_files/TMPA-to-IMERG\\_transition.pdf](https://pmm.nasa.gov/sites/default/files/document_files/TMPA-to-IMERG_transition.pdf). Accessed 15 Aug 2017
- Huffman GJ, Pendergrass A, National Center for Atmospheric Research Staff (eds) (2017). The climate data guide: TRMM: tropical rainfall measuring mission. <https://climatedataguide.ucar.edu/climate-data/trmm-tropical-rainfall-measuring-mission>. Accessed 06 Jan 2017
- Ioannidou A, Papastefanou C (2006) Precipitation scavenging of  $^7\text{Be}$  and  $^{137}\text{Cs}$  radionuclides in air. *J Environ Radioact* 85(1):121–136. <https://doi.org/10.1016/j.jenvrad.2005.06.005>
- Kaste JM, Norton SA, Hess CT (2002) Environmental chemistry of Beryllium-7. *J Rev Mineral Geochem* 50:271–289. <https://doi.org/10.2138/rmg2002506>
- Kaste JM, Elmore AJ, Vest KR, Okin GS (2011) Beryllium-7 in soils and vegetation along an arid precipitation gradient in Owens Valley, California, Geophys. Res Lett 38:L09401. <https://doi.org/10.1029/2011GL047242>
- Lal D, Malhotra PK, Peters B (1958) On the production of radioisotopes in the atmosphere by cosmic radiation and their application to meteorology. *J Atmos Terrestrial Phys* 12(4):306–328. [https://doi.org/10.1016/0021-9169\(58\)90062-X](https://doi.org/10.1016/0021-9169(58)90062-X)
- Lohaiza F, Velasco H, Juri Ayub J, Rizzotto M, Di Gregorio DE, Huck H, Valladares DL (2014) Annual variation of  $^7\text{Be}$  soil inventory in a semiarid region of central Argentina. *J Environ Radioact* 130:72–77. <https://doi.org/10.1016/j.jenvrad.2014.01.006>
- Magliano PN, Fernández RJ, Mercu JL, Jobbágy EG (2015) Precipitation event distribution in Central Argentina: spatial and temporal patterns. *Ecohydrology* 8:94–104. <https://doi.org/10.1002/eco.1491>
- Matissoff G, Bonniwell EC, Whiting PJ (2002) Soil erosion and sediment sources in an Ohio watershed using Beryllium-7, Cesium-137 and Lead-210. *J Environ Qual* 31:54–61. <https://doi.org/10.2134/jeq2002.5400>
- Nachtergaele FO, Petri M, Biancalani R, van Lynden G, van Velthuisen H, Bloise M (2011) Global land degradation information system (GLADIS). An information database for land degradation assessment at global level. Technical working paper of the LADA FAO/UNEP project
- Papastefanou C (2006) Residence time of tropospheric aerosols in association with radioactive nuclides. *Appl Radiat Isot* 64:93–100. <https://doi.org/10.1016/j.apradiso.2005.07.006>
- Papastefanou C, Ioannidou A (2004). Beryllium-7 and solar activity. *Appl Radiat Isot* 61(6):1493–1495. <https://doi.org/10.1029/2000GL003792>
- Perillo Isaac MC, Hurley D, McDonald RJ, Norman EB, Smith A (1997) A natural calibration source for determining germanium detector efficiencies. *Nucl Instrum Methods Phys Res A* 397:310–316
- Piñero García F, Ferro García MA (2013) Evolution and solar modulation of  $^7\text{Be}$  during the solar cycle 23. *J Radioanal Nucl Chem* 296:1193–1204. <https://doi.org/10.1007/s10967-012-2373-y>
- REM (2017) Red de Estaciones Meteorológicas. <http://www.clima.sanluis.gov.ar/InformePorPeriodo.aspx>. Accessed 10 Mar 2017
- Salisbury RT, Cartwright J (2005) Cosmogenic  $^7\text{Be}$  deposition in North Wales:  $^7\text{Be}$  concentrations in sheep faeces in relation to altitude and precipitation. *J Environ Radioact* 78:353–361. <https://doi.org/10.1016/j.jenvrad.2004.05.013>
- Schuller P, Iroume A, Walling D, Mancilla H, Castillo A, Trumper R (2006) Use of  $^7\text{Be}$  to document soil redistribution following forest harvest operations. *J Environ Qual* 35:1756–1763. <https://doi.org/10.2134/jeq2005.0410>
- Sepulveda A, Schuller P, Walling DE, Castillo A (2008) Use of  $^7\text{Be}$  to document soil erosion associated with a short period of extreme rainfall. *J Environ Radioact* 99:35–49. <https://doi.org/10.1016/j.jenvrad.2007.06.010>
- Steinmann P, Billen T, Loizeau JL, Dominik J (1999) Beryllium-7 as a tracer to study mechanism and rates of metal scavenging from lake surface waters. *Geochim Cosmochim Acta* 63:1621–1633. [https://doi.org/10.1016/S0016-7037\(99\)00021-6](https://doi.org/10.1016/S0016-7037(99)00021-6)
- Van Allen J (2000) On the modulation of galactic cosmic ray intensity during solar activity cycles 19, 20, 21, 22 and early 23. *Gephys Res Lett* 27:2453–2456 <https://doi.org/10.1016/j.jastp.2007.10.001>
- Wallbrink PJ, Murray AS (1994) Fallout of  $^7\text{Be}$  in South Eastern Australia. *J Environ Radioact* 25:213–228. [https://doi.org/10.1016/0265-931X\(94\)90074-4](https://doi.org/10.1016/0265-931X(94)90074-4)
- Walling DE, He Q, Blake W (1999) Use of  $^7\text{Be}$  and  $^{137}\text{Cs}$  measurements to document short- and medium-term rates of water-induced soil erosion on agricultural land. *Water Resour Res* 35:3865–3874. <https://doi.org/10.1029/1999WR900242>
- Walling DE, Schuller P, Zhang Y, Iroume A (2009) Extending the timescale for using Beryllium-7 measurements to document soil redistribution by erosion. *Water Resour Res*. <https://doi.org/10.1029/2008WR007143>
- Yoshimori M (2005) Production and behavior of Beryllium-7 radionuclide in the upper atmosphere. *Adv Sp Res* 36:922–926. <https://doi.org/10.1016/j.asr.2005.04.093>
- Zapata F (2002) Handbook for assessment of soil erosion and sedimentation using environmental radionuclides. Kluwer, Dordrecht